Renormalized single-particle properties in a spin density wave antiferromagnet

W. Brenig, Arno P. Kampf

Angaben zur Veröffentlichung / Publication details:

Brenig, W., and Arno P. Kampf. 1993. "Renormalized single-particle properties in a spin density wave antiferromagnet." *Europhysics Letters (EPL)* 24 (8): 679–85. https://doi.org/10.1209/0295-5075/24/8/010.

Renormalized Single-Particle Properties in a Spin Density Wave Antiferromagnet.

W. BRENIG(*) and A. P. KAMPF(**)

(*) *Institut für Theoretische Physik, Universität zu Köln*
Zülpicher Str. 77, 50937 Köln, Germany
(**) *Institut für Festkörperforschung, Forschungszentrum Jülich*
52425 Jülich, Germany

Abstract. – We present a self-consistent strong-coupling scheme to evaluate the single-particle Green's function for the two-dimensional Hubbard model in the spin density wave state. We analyse the single–quasi-hole properties including its dispersion and spectral weight. Novel incoherent contributions to the spectral function resulting from multi–spin-wave processes are found and compared to similar results for the *t-J* model and small Hubbard clusters.

Introduction. – The vicinity of antiferromagnetism and superconductivity in the layered high-temperature superconductors has stimulated research to understand the properties of carriers doped into an antiferromagnetic (AF) insulating state in two dimensions. In strong-coupling approaches the competition between AF ordering of localized-spin degrees of freedom and the delocalization of doped holes is the key issue. For the *t-J* model exact diagonalization [1, 2], cumulant [3], and spin polaron methods [4] have given evidence that a quasi-particle picture for the coherent motion of a hole is still applicable. However, a significant reduction of the quasi-particle weight and a correspondingly large redistribution of spectral intensity into the incoherent part of the single-particle propagator is found in all these studies. Similar results are reported for the Hubbard model in the intermediate–to–strong-coupling regime [5, 6].

Less extensively studied are the elementary excitations in the weak-coupling limit of the Hubbard model. In this case the spin density wave (SDW) state can be taken as a starting point to explore the single-particle dynamics. In this letter we will focus on the properties of a single hole doped into the SDW state. In this case the hole motion is accompanied by multi–spin-wave excitation processes which reduce the quasi-hole's spectral weight and strongly renormalize the bandwidth and the single-particle gap. The quasi-hole's dispersion is found to be very flat along the magnetic-Brillouin-zone (MBZ) boundary contrary to results obtained for the *t-J* model.

SDW *spin dynamics*. – The starting point for our calculations is the SDW representation of the Hubbard model on a square lattice at half-filling [7]

$$H = \sum_{k\sigma,\, l=\pm 1}{}' \, l E_k a^{l\dagger}_{k\sigma} a^{l}_{k\sigma} + H_U . \tag{1}$$

Here, $a^{l\dagger}_{k\sigma}$ creates a SDW quasi-particle in the conduction or valence band for $l = +1$ or -1, respectively, and H_U is the residual Hubbard interaction. The mean-field dispersion for the upper and lower SDW band is given by $E_k = \pm\sqrt{\varepsilon_k^2 + \Delta^2}$ in terms of the tight-binding energy $\varepsilon_k = -2t(\cos(k_x a) + \cos(k_y a))$ and the magnetic SDW energy gap Δ. The primed summation is restricted to the MBZ. The magnitude of Δ follows from the gap equation $1/U = (1/N)\sum_k{}' 1/E_k$ which is the Hartree-Fock(HF) self-consistency condition for the staggered magnetization $\langle S_z(\boldsymbol{Q})\rangle$ in the broken-symmetry state. $\boldsymbol{Q} = (\pi, \pi)$ is the square lattice nesting wave vector. Due to the doubling of the unit cell the SDW quasi-particles are restricted to the MBZ, *i.e.* to momenta where $\varepsilon_k < 0$. They are related to the bare-fermion operators $c^{l\dagger}_{k\sigma}$ of the original Hubbard model by the linear transformation $a^{l\dagger}_{k\sigma} = v^l_k c^\dagger_{k\sigma} + l\sigma v_k^{-l} c^\dagger_{k+Q\sigma}$ with $v^l_k = [(1 + l\varepsilon_k/E_k)/2]^{1/2}$. To facilitate the transformation to physical operators the SDW quasi-particles are extended to the Brillouin zone (BZ) by the prescription $a^{l\dagger}_{k\sigma} = l\sigma a^\dagger_{k-Q\sigma}$ leading to the modified fermionic algebra $[a^l_{k\sigma}, a^{l'\dagger}_{k'\sigma'}]_+ = \delta_{ll'}\,\delta_{\sigma\sigma'}(\delta_{kk'} + l\sigma\delta_{kk'+Q})$. This formal step allows to express $c^\dagger_{k\sigma} = \sum_{l=\pm 1} v^l_k a^{l\dagger}_{k\sigma}$ for *all* $\boldsymbol{k} \in$ BZ.

The broken spin rotational invariance of the SDW state implies the existence of gapless collective spin excitations. In order to calculate these Goldstone modes we consider the transverse dynamical spin susceptibility

$$\chi^{+-}(\boldsymbol{q}, \boldsymbol{q}', t) = i\langle T S^+_{\boldsymbol{q}}(t) S^-_{\boldsymbol{q}'}(0)\rangle \tag{2}$$

including Gaussian fluctuations around the HF ground state. $\chi^{+-}(\boldsymbol{q}, \boldsymbol{q}', \omega)$ is a symmetric 2×2 matrix with respect to the momentum indices since it is finite only if $\boldsymbol{q} = \boldsymbol{q}'$ or $\boldsymbol{q} = \boldsymbol{q}' \pm \boldsymbol{Q}$ due to Umklapp scattering. Summing the RPA bubble series leads to

$$\chi^{+-}_{\text{RPA}}(\boldsymbol{q}, \boldsymbol{q}', \omega) = \sum_{\tilde{\boldsymbol{q}}} \chi_0(\boldsymbol{q}, \tilde{\boldsymbol{q}}, \omega)[1 - U\chi_0(\tilde{\boldsymbol{q}}, \boldsymbol{q}', \omega)]^{-1}, \tag{3}$$

where $[1 - U\chi_0(\tilde{\boldsymbol{q}}, \boldsymbol{q}', \omega)]^{-1}$ is a matrix inverse in momentum space. The bare particle-hole susceptibility χ_0 is calculated with the HF c-electron propagator matrix whose diagonal and off-diagonal components are given by

$$\begin{bmatrix} G^{0c}_\sigma(\boldsymbol{k}, \boldsymbol{k}, \omega) \\ G^{0c}_\sigma(\boldsymbol{k}+\boldsymbol{Q}, \boldsymbol{k}, \omega) \end{bmatrix} = \frac{1}{\omega^2 - E_k^2 + i\eta} \begin{bmatrix} \omega + \varepsilon_k \\ \sigma\Delta \end{bmatrix}. \tag{4}$$

The corresponding matrix elements of χ_0 are

$$\begin{bmatrix} \chi_0(\boldsymbol{q}, \boldsymbol{q}, \omega) \\ \chi_0(\boldsymbol{q}+\boldsymbol{Q}, \boldsymbol{q}, \omega) \end{bmatrix} = \sum_k{}' \frac{2}{\omega^2 - (E_k + E_{k+q})^2 + i\eta} \begin{bmatrix} -(E_k + E_{k+q})\, m^2_{k,k+q} \\ \omega l_{k,k+q} m_{k,k+q} \end{bmatrix}. \tag{5}$$

In (5) we have introduced the coherence factors $m_{k,k'} = v^+_k v^-_{k'} + v^-_k v^+_{k'}$ and $l_{k,k'} = v^+_k v^+_{k'} + v^-_k v^-_{k'}$. To extract the collective spin dynamics we resort to a strong-coupling expansion assuming $U \gg t$. This procedure has previously been shown [7] to reproduce the results of linear–spin-wave theory for the 2D AF Heisenberg model of localized spins with an exchange constant $J = 4t^2/U$. The analysis of [7] can also be extended to finite doping [8, 9] but in this

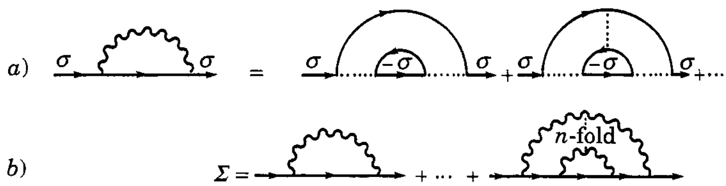

Fig. 1*a*). – Self-energy correction from the coupling to transverse spin fluctuations in the RPA ladder series. *b*) NC scheme for the self-energy. The wiggly line represents the RPA ladder series of *a*).

letter we concentrate on the half-filled case. The transverse susceptibility in this limit explicitly displays undamped propagating spin waves:

$$\begin{bmatrix} \chi_{\mathrm{RPA}}^{\bar\sigma-\bar\sigma}(\boldsymbol{q},\boldsymbol{q},\omega) \\ \chi_{\mathrm{RPA}}^{\bar\sigma-\bar\sigma}(\boldsymbol{q}+\boldsymbol{Q},\boldsymbol{q},\omega) \end{bmatrix} \xrightarrow{U/t\gg 1} \frac{1}{\omega^2-\omega_q^2+i\eta} \begin{bmatrix} -2J(1+\varepsilon_q/4t) \\ \sigma\omega \end{bmatrix} \equiv \begin{bmatrix} \chi_S^{\bar\sigma-\sigma}(\boldsymbol{q},\boldsymbol{q},\omega) \\ \chi_S^{\bar\sigma-\sigma}(\boldsymbol{q}+\boldsymbol{Q},\boldsymbol{q},\omega) \end{bmatrix} \tag{6}$$

with the spin wave dispersion $\omega_q = 2J\sqrt{1-(\varepsilon_q/4t)^2}$ and $\sigma = \pm 1$. The coupling to these low-energy spin wave modes is assumed to be the dominant source for the renormalization of the single-particle properties. We will go beyond previously applied lowest-order one-loop calculations [9-11] and evaluate the electronic self-energy in a self-consistent non-crossing (NC) scheme.

AF *polarons in the* SDW *state.* – We focus on the renormalization effects due to *multiple*–spin-wave shake-offs. For this purpose we consider the Dyson equation for the single-particle propagator which arises from the exchange of a *single* RPA ladder carrying the spin wave excitation. This is shown diagrammatically in fig. 1*a*). Using the *c*-electron representation of the Hubbard model the self-energy is expressed as

$$\Sigma_\sigma^c(\boldsymbol{k}_1,\boldsymbol{k}_2,i\varepsilon_\mu) = -TU^2\sum_{\boldsymbol{q},\omega_\nu}[G_{-\sigma}^{0c}(\boldsymbol{k}_1-\boldsymbol{q},\boldsymbol{k}_2-\boldsymbol{q},i\varepsilon_\mu-i\omega_\nu)\chi_{\mathrm{RPA}}^{-\bar\sigma\bar\sigma}(\boldsymbol{q},\boldsymbol{q},i\omega_\nu)+$$
$$+G_{-\sigma}^{0c}(\boldsymbol{k}_1+\boldsymbol{Q}-\boldsymbol{q},\boldsymbol{k}_2-\boldsymbol{q},i\varepsilon_\mu-i\omega_\nu)\chi_{\mathrm{RPA}}^{-\bar\sigma\bar\sigma}(\boldsymbol{q}+\boldsymbol{Q},\boldsymbol{q},i\omega_\nu)]. \tag{7}$$

Here we use the standard finite-temperature notation where $\omega_\nu = 2\nu\pi T$ and $\varepsilon_\mu = (2\mu+1)\pi T$ are Matsubara frequencies. Accounting for all possible Umklapp contractions (7) consists of four equations in which each of the two momentum vectors $\boldsymbol{k}_1$ and $\boldsymbol{k}_2$ takes on only the two values $\boldsymbol{k}$ and $\boldsymbol{k}+\boldsymbol{Q}$, respectively. The two terms on the r.h.s. denote the allowed internal combinations of momenta compatible with the Umklapp vector $\boldsymbol{Q}$.

The motion of the SDW quasi-particles is expected to be strongly coupled to the spin wave excitations. Therefore, instead of the single RPA boson exchange we replace the bare propagator G_σ^{0c} in eq. (7) by the *fully dressed* Green's function G_σ^c. Diagrammatically this procedure is equivalent to a summation of all NC diagrams for the self-energy as shown in fig. 1*b*). This replaces eq. (7) by a set of four non-linear coupled integral equations for the single-particle propagators.

To reduce the mathematical complexity of the NC equations, we introduce two simplifications: firstly, the formal limit of $U \gg t$ is taken using the transverse spin susceptibility in the form given in eq. (6) and replacing the transformation coefficients v_k^l by their large U value, *i.e.* $1/\sqrt{2}$. Secondly, we consider a *single hole* which is inserted into the SDW state at half-filling. This approximation should properly describe the case of very low doping. In this limit we transform from the *c*-fermion to the *a*-fermion representation. After some elementary algebra the strong-coupling version of the NC equations takes on the simple form

$$\Sigma_\sigma^{ll}(\boldsymbol{k}, i\varepsilon_\mu) = -TU^2 \sum_{\boldsymbol{q},\,\omega_\nu}{}' [\chi_S^{\bar\sigma\sigma}(\boldsymbol{q}, \boldsymbol{q}, i\omega_\nu) + \chi_S^{\bar\sigma\sigma}(\boldsymbol{q}+\boldsymbol{Q}, \boldsymbol{q}+\boldsymbol{Q}, i\omega_\nu) + $$

$$+ l\sigma 2\chi_S^{\bar\sigma\sigma}(\boldsymbol{q}+\boldsymbol{Q}, \boldsymbol{q}, i\omega_\nu)]\, G_{-\sigma}^{-l\;-l}(\boldsymbol{k}-\boldsymbol{q}, i\varepsilon_\mu - i\omega_\nu)\,, \qquad (8)$$

$$\Sigma_\sigma^{-l\;l}(\boldsymbol{k}, i\varepsilon_\mu) = -TU^2 \sum_{\boldsymbol{q},\,\omega_\nu}{}' [\chi_S^{\bar\sigma\sigma}(\boldsymbol{q}, \boldsymbol{q}, i\omega_\nu) - $$

$$-\chi_S^{\bar\sigma\sigma}(\boldsymbol{q}+\boldsymbol{Q}, \boldsymbol{q}+\boldsymbol{Q}, i\omega_\nu)]\, G_{-\sigma}^{l\;-l}(\boldsymbol{k}-\boldsymbol{q}, i\varepsilon_\mu - i\omega_\nu)\,, \qquad (9)$$

where $\Sigma_\sigma^{ll'}(\boldsymbol{k}, i\varepsilon_\mu)$ and $G_\sigma^{ll'}(\boldsymbol{k}, i\varepsilon_\mu)$ are the momentum diagonal components of the a-fermion self-energy and the *dressed* a-Green's function for band indices $l, l' = \pm 1$.

Starting from the HF propagator the iterative solution of eq. (9) leads to a vanishing *interband* self-energy and a vanishing *interband* Green's function. This leaves only the two equations (8) for the *intraband* Green's function to be solved. Since both the kernel of this integral equation and the bare SDW Green's functions are spin independent, one may replace $G_{-\sigma}^{ll}$ by G_σ^{ll} on the r.h.s. of eq. (8). Finally, in the limit of a single hole introduced into the SDW ground state our model is particle-hole symmetric [10]. This is reflected by the symmetry relation for the spectral functions $A_\sigma^{-1\;-1}(\boldsymbol{k}, \omega) = A_\sigma^{11}(\boldsymbol{k}, -\omega)$, where $A_\sigma^{ll}(\boldsymbol{k}, \omega) = -\mathrm{Im}[G_\sigma^{ll}(\boldsymbol{k}, \omega + i\eta)]/\pi$. Indeed, explicit insertion of this particle-hole transformation into (3.2) verifies that the two equations are equivalent.

We are thus left with only a single integral equation, *e.g.* for the valence band propagator. We perform the necessary frequency summations and proceed via an analytic continuation to

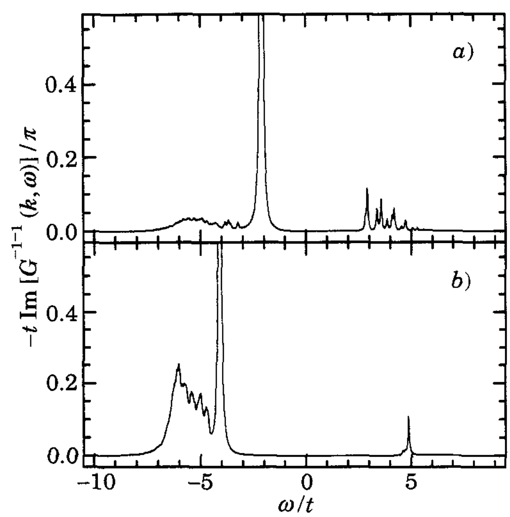

Fig. 2.

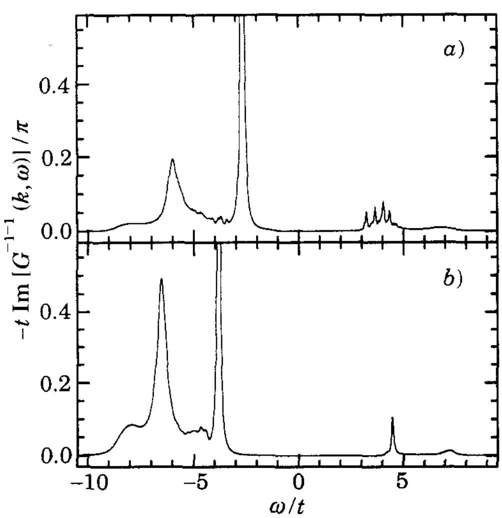

Fig. 3.

Fig. 2. – Single-hole spectral function for $U = 4$ and the two momenta $(k_x, k_y) = (0, 0)$ (a)) and $(k_x, k_y) = (\pi/2, \pi/2)$ (b)) on a 16×16 lattice. Energies are given in units of t.

Fig. 3. – Same as in fig. 2 for $U = 6$.

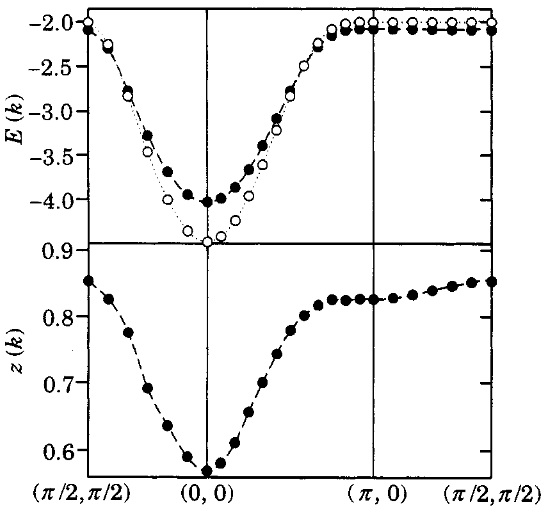

Fig. 4.

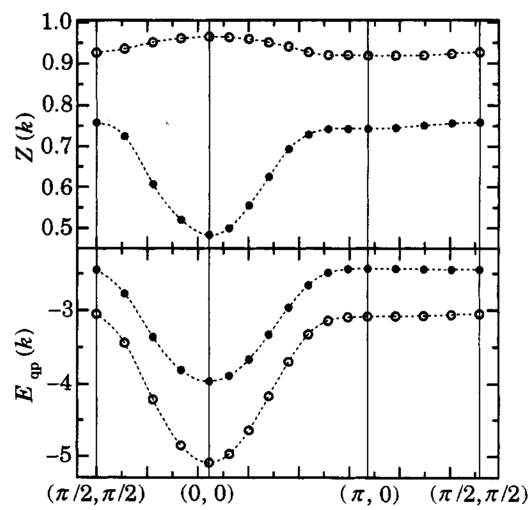

Fig. 5.

Fig. 4. – Quasi-particle properties for $U = 4$ on a 24×24 lattice along a closed triangular path in the MBZ. The upper panel shows the NC quasi-particle dispersion (●) as compared to the SDW dispersion (○) $E(\boldsymbol{k})$ for $2\Delta = U$. The lower panel shows the corresponding quasi-particle weight factor.

Fig. 5. – Comparison of the quasi-particle properties for $U = 4$ in a 16×16 lattice resulting from a single iteration of eq. (10), *i.e.* the one-loop level (○), *vs.* the NC (●) solution.

the retarded quantities. In the zero-temperature limit we obtain

$$\Sigma_{\sigma}^{-1\ -1}(\boldsymbol{k}, z) = U^2 {\sum_{\boldsymbol{q} \neq 0}}' \left\{ \left(1 + \frac{2J}{\omega_{\boldsymbol{q}}}\right) \int_0^{\infty} d\omega' \, \frac{A_{\sigma}^{-1\ -1}(\boldsymbol{k} - \boldsymbol{q}, \omega')}{\omega_{\boldsymbol{q}} + \omega' + z} + \right.$$
$$\left. + \left(1 - \frac{2J}{\omega_{\boldsymbol{q}}}\right) \int_{-\infty}^{0} d\omega' \, \frac{A_{\sigma}^{-1\ -1}(\boldsymbol{k} - \boldsymbol{q}, \omega')}{\omega_{\boldsymbol{q}} - \omega' - z} \right\}, \tag{10}$$

where $z = \omega + i\eta$. This expression represents the central equation for our self-consistent treatment of a spin polaron in the SDW state.

Results and discussion. – We have solved eq. (10) by iteration on finite lattices up to 24×24 sites. The frequency mesh size was on the order of 1000–2000 points. Typically up to 20 iterations were necessary to obtain convergence. In all calculations an imaginary part $i\eta$ of 1/2 of the frequency spacing was introduced as an artificial broadening.

Results for the single-hole spectral function are shown in fig. 2 and 3 for the two momenta $(k_x, k_y) = (\pi/2, \pi/2)$ and $(k_x, k_y) = (0, 0)$ on a 16×16 sites lattice. Two moderate values for the Hubbard U have been chosen which, however, still justify the use of the strong-coupling limit in the self-consistent NC polaron scheme. Besides the renormalization of the quasi-hole peak the figures display a considerable shift of spectral weight into a spin wave shake-off structure below the quasi-hole energy and into the upper Hubbard band. Similar incoherent spectral weight is found in the one-hole spectrum of the t-J model only on the low-energy side of the quasi-hole peak, since the upper Hubbard band is removed by the strict exclusion of

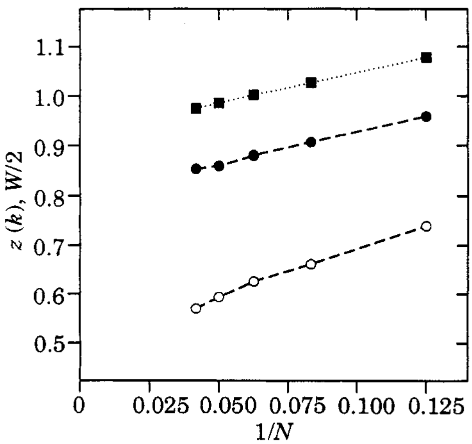

Fig. 6. – Finite-size scaling for the quasi-particle weight factors $z((\pi/2,\ \pi/2))$ and $z((0,\ 0))$ and for half of the valence bandwidth $W/2$. N is the linear lattice size, $U = 4$.

doubly occupied sites. This is the result of both exact diagonalization studies and approximate NC calculations [4]. On the other hand the incoherent low-energy continuum is missing in earlier calculations which have been performed in the SDW state using only a one-loop approximation [10]. This approach lacks the relevant transfer of spectral weight resulting from the multiple–spin-wave excitations. In this sense our self-consistent polaron scheme interpolates between these two limits. But the physical situation in both cases is quite different. In the *t-J* limit of the Hubbard model a spin wave emission leads to mobility of a hole inserted into the AF ordered background while in the SDW case spin waves cause a mass enhancement of the SDW quasi-particles.

The loss of spectral weight into the incoherent part is much stronger for the zone centre holes than for holes on the boundary of the MBZ. This behaviour is made more explicit in fig. 4 which shows the quasi-hole's spectral weight factor $z(\boldsymbol{k})$ and its dispersion for momenta along a closed path in the MBZ. A comparison to the HF SDW dispersion demonstrates the significant band narrowing of the polaron band. Most striking is the result that the degeneracy of the HF bands along the MBZ boundary is barely lifted. Although not clearly visible in the figure the energy maximum of the quasi-particle band occurs at $\boldsymbol{k} = (\pi,\ 0)$. This is a result which arises only on the multiloop level, since for the one-loop calculation the maximum does appear at $\boldsymbol{k}_p = (\pi/2,\ \pi/2)$ [10].

While it seems generally accepted for the *t-J* model that the maximum is at $\boldsymbol{k}_p = (\pi/2,\ \pi/2)$, this issue is much more subtle for the Hubbard model. Quantum Monte Carlo calculations on small clusters with finite hole concentrations have found no evidence for hole pockets near $\boldsymbol{k}_p$ and a Fermi surface whose shape is hardly changed when compared to the Fermi surface of the non-interacting tight-binding band [12]. Lanczos diagonalization studies on a 4×4 Hubbard cluster have found near degeneracy between $\boldsymbol{k}_p$ and $(\pi,\ 0)$ but in slight favour for the maximum to occur at $(\pi,\ 0)$ [5] in agreement with the self-consistent NC calculation.

The differences between the one-loop and the self-consistent NC calculation are demonstrated in fig. 5 which shows the large changes in the bandwidth and the quasi-hole's spectral weight near the centre of the MBZ. The upward shift of the valence quasi-particle band (and the analogous downward shift of the conduction band) also reveals the strong renormalization of the band gap. Interestingly, the gap is reduced in the self-consistent NC scheme while it even grows on the one-loop level. Moreover, we find a non-linear dependence of the effective gap on the Hubbard U when it is increased beyond $U = 6t$. This signals that vertex corrections which renormalize the bare coupling to an effective U_{eff} need to be included in this regime.

The effects of finite lattice sizes are shown in fig. 6, where the spectral-weight factors for different momenta and the width of the valence band are plotted *vs.* the inverse linear size of the lattice. Both scale approximately inversely proportional to the linear size of the lattice. Quantitatively, *e.g.* for $U = 4t$, the bandwidth extrapolates to $W = 1.85t$ as compared to the SDW bandwidth $W_{\text{SDW}} = 2.81t$ and the spectral-weight factors extrapolate to $z((\pi/2, \pi/2)) = 0.8$ and $z((0, 0)) = 0.51$ in the infinite lattice limit.

In conclusion we have analysed the single-particle properties in the SDW state using a non-crossing scheme. A straightforward extension to the weak-coupling limit and an analysis for the renormalization of the spin wave excitations is currently in progress.

* * *

The authors are grateful to Profs. K.W. Becker, P. Fulde and E. Müller-Hartmann for helpful discussions. This work has been performed within the program of the Sonderforschungsbereich 341 supported by the Deutsche Forschungsgemeinschaft.

REFERENCES

[1] Dagotto E., Joynt R., Moreo A., Bacci S. and Gagliano E., *Phys. Rev. B*, **41** (1990) 9049.
[2] Stephan W. and Horsch P., *Phys. Rev. B*, **66** (1991) 2258.
[3] Eder R. and Becker K. W., *Z. Phys. B*, **78** (1990) 219.
[4] Martinez G. and Horsch P., *Phys. Rev. B*, **44** (1991) 317; Ramšak A. and Prelovšek P., *Phys. Rev. B*, **42** (1990) 10415; Furukawa N. and Imada M., *J. Phys. Soc. Jpn.*, **59** (1990) 1771; Igarashi J. and Fulde P., *Phys. Rev. B*, **45** (1992) 12357; Liu Z. and Manousakis E., *Phys. Rev. B*, **45** (1992) 2425.
[5] Leung P. W., Liu Z., Manousakis E., Novotny M. A. and Oppenheimer P. E., *Phys. Rev. B*, **46** (1992) 11779.
[6] Dagotto E., Ortolani F. and Scalapino D. J., *Phys. Rev. B*, **46** (1992) 3183.
[7] Schrieffer J. R., Wen X. G. and Zhang S. C., *Phys. Rev. B*, **39** (1989) 11663.
[8] Brenig W., Kampf A. P. and Becker K. W., unpublished.
[9] Chubukov A. V. and Frenkel D. M., *Phys. Rev. B*, **46** (1992) 11884.
[10] Vignale G. and Hedayati M. R., *Phys. Rev. B*, **42** (1990) 786.
[11] Singh A. and Tešanović Z., *Phys. Rev. B*, **41** (1990) 614.
[12] Moreo A., Scalapino D. J., Sugar R. L., White S. R. and Bickers N. E., *Phys. Rev. B*, **41** (1990) 2313.